



## Adsorption of Co(II) ions from aqueous solutions using NiFe<sub>2</sub>O<sub>4</sub> nanoparticles

Soheil Sobhanardakani<sup>1</sup>, Raziyeh Zandipak<sup>2</sup>

1 Department of Environment, Hamadan Branch, Islamic Azad University, Hamadan, Iran

2 Young Researchers and Elite Club, Hamadan Branch, Islamic Azad University, Hamadan, Iran

### Original Article

#### Abstract

In this study, NiFe<sub>2</sub>O<sub>4</sub> nanoparticles (NiFe<sub>2</sub>O<sub>4</sub> NPs) were prepared through co-precipitation method and subsequently used for the removal of Co(II) ions from aqueous solutions. The NiFe<sub>2</sub>O<sub>4</sub> NPs were characterized by transmission electron microscopy (TEM), X-ray diffraction spectrometry (XRD), and Brunauer-Emmett-Teller (BET) surface area analysis. In batch tests, the effects of variables such as pH (2-10), adsorbent dose (0.006-0.08 g), contact time (0-90 minutes), and temperature (25-55 °C) on Co(II) ions removal were examined and optimized values were found to be 7, 0.02 g, 70 minutes, and 25 °C, respectively. In addition, the experimental data were fitted well to the Langmuir isotherm model and the maximum adsorption capacity was found to be 322.5 mg/g. Kinetic experiments were also conducted to determine the rate at which Co(II) ions are adsorbed onto the NiFe<sub>2</sub>O<sub>4</sub> NPs.

**KEYWORDS:** Cobalt, Removal, Nanoparticles, Kinetics

**Date of submission:** 17 Apr 2015, **Date of acceptance:** 22 Jun 2015

**Citation:** Sobhanardakani S, Zandipak R. **Adsorption of Co(II) ions from aqueous solutions using NiFe<sub>2</sub>O<sub>4</sub> nanoparticles.** J Adv Environ Health Res 2015; 3(3): 179-87.

#### Introduction

Cobalt contamination in natural waters is the cause of worldwide environmental concern since cobalt-polluted water can pose a great risk to human health due to its high toxicity.<sup>1,2</sup> The main anthropogenic pathway through which Co(II) enters water is via wastewaters from various industrial processes such as nuclear power plants, and metallurgical, mining, and electronic industries and pigments and paints.<sup>3,4</sup> Everyone is exposed to low levels of Co(II) present in air, water, and food. The permissible limits of Co in irrigation water and live-stock watering are 0.05 and 1.0 mg/l, respectively.<sup>2</sup> Small amounts of Co(II) is essential for human health, because it is known

to be an essential element at trace levels in human beings, animals, and plants for metabolic processes.<sup>4</sup> Although Co(II) is essential for humans, large amounts of it can cause paralysis, diarrhea, asthma, pneumonia, lung irritations, weight loss, vomiting, nausea, and damage to the thyroid and liver.<sup>5</sup> Various treatment technologies for the removal of Co(II), such as precipitation, coagulation, ion exchange, biological treatment, and chemical reduction, have limited applications because of their relatively high cost and the production of secondary pollution.<sup>6-9</sup> Adsorption is an effective and economic method for the removal of heavy metals from wastewaters.<sup>10-12</sup> Activated carbon, zeolites, natural clays, chitosan, and by-products have been used as adsorbents for removal of metals from wastewaters.<sup>13-15</sup>

#### Corresponding Author:

Raziyeh Zandipak

Email: raziye.zandi@yahoo.com

Recently, magnetic nanomaterials have attracted much interest, because they not only have a large removal capacity, fast kinetics, and reactivity for contaminant removal, but also have high separation efficiency and reusability. In recent years, magnetic nanoparticles (NPs) with the general formula of MFe<sub>2</sub>O<sub>4</sub> (M = Fe, Co, Cu, Mn, Ni, and etc.) have been among the most popular materials in analytical biochemistry, medicine, removal of heavy metals, and biotechnology.<sup>16</sup> Moreover, they have been increasingly applied to immobilize proteins, enzymes, and other bioactive agents due to their unique advantages.<sup>16</sup>

NiFe<sub>2</sub>O<sub>4</sub> nanoparticles (NiFe<sub>2</sub>O<sub>4</sub> NPs) are recognized as an adsorbent because of their good biocompatibility, strong super paramagnetic property, low toxicity, easy preparation, and high adsorption capacity.<sup>17</sup> NiFe<sub>2</sub>O<sub>4</sub> NPs with an inverse spinel structure show ferrimagnetism that originates from the magnetic moment of antiparallel spins between Fe<sup>3+</sup> ions at tetrahedral sites and Ni<sup>2+</sup> ions at octahedral sites. NiFe<sub>2</sub>O<sub>4</sub> NPs exhibit high surface area and low mass transfer resistance. Moreover, the magnetic behavior of these nanoparticles depends mostly on their size.<sup>18</sup>

In this study, the removal of Co(II) ions from aqueous solutions using NiFe<sub>2</sub>O<sub>4</sub> NPs has been described. Effects of various parameters such as pH of the solutions, amount of adsorbent, contact time, and temperature were investigated. In addition, isotherm and kinetic studies of Co(II) ions removal in batch system were carried out.

## Materials and Methods

All chemicals and reagents used in this work were of analytical grade and purchased from Merck Company (Merck, Darmstadt, Germany). A stock solution of Co(II) (1000 mg/l) was prepared by dissolving Co(NO<sub>3</sub>)<sub>2</sub>·6H<sub>2</sub>O in double-distilled water.

The concentration of Co(II) ions in the solution was measured using an inductively coupled plasma optical emission spectrometer

(ICP-OES) (JY138 Ultrace, France). All pH measurements were conducted with a 780 pH meter (780, Metrohm, Switzerland) combined with a glass-calomel electrode.

The crystal structure of synthesized materials was determined through X-ray powder diffraction (XRD) (38066 Riva, d/G.Via M. Misone, 11/D (TN), Italy) at ambient temperature. The structure of the NiFe<sub>2</sub>O<sub>4</sub> NPs was characterized using a transmission electronic microscope (TEM) (CM10, 100 KV, Philips, Eindhoven, Netherlands). Specific surface area and porosity were defined through N<sub>2</sub> adsorption-desorption porosimetry (77 K) using a porosimeter (Bel Japan, Inc.). The elemental analysis was conducted using a scanning electron microscope energy dispersive X-ray spectroscope (SEM-EDX, XL 30, Philips, Netherland).

The NiFe<sub>2</sub>O<sub>4</sub> samples were prepared through co-precipitation method. In a typical synthesis, 0.2 M (20 ml) solution of iron nitrate [(Fe(NO<sub>3</sub>)<sub>3</sub>·9H<sub>2</sub>O)] and 0.1 M (20 ml) solution of nickel nitrate [(Ni(NO<sub>3</sub>)<sub>2</sub>·6H<sub>2</sub>O)] were prepared and vigorously mixed through stirring for 1 hour at 80 °C. Then, 0.2 g of polyethylene oxide (PEO) was added to the solution as a capping agent. Subsequently, 5 ml of hydrazine hydrate (NH<sub>2</sub>·NH<sub>2</sub>·H<sub>2</sub>O) was added drop by drop to the solutions and brown-colored precipitates were formed. Finally, the precipitates were separated through centrifugation and dried in a hot air oven for 4 hours at 100 °C. The acquired substance was annealed for 10 hours at 300 °C.<sup>19</sup>

The point of zero charge pH (pH<sub>pzc</sub>) for the adsorbents was determined by introducing 0.02 g of NiFe<sub>2</sub>O<sub>4</sub> NPs into 8 Erlenmeyer flasks (100 ml) containing 0.1 M NaNO<sub>3</sub> solution. The pH values of the solutions were adjusted to 2, 3, 4, 5, 6, 7, 8, and 9 using solutions of 0.01 mol/l HNO<sub>3</sub> and NaOH. The solution mixtures were allowed to equilibrate in an isothermal shaker (25 °C) for 24 hours. The final pH was measured after 24 hours. The pH<sub>pzc</sub> is the point at which the pH<sub>initial</sub> is equal to pH<sub>final</sub>.<sup>19</sup>

To perform an adsorption isotherm analysis, adsorption experiments were carried out by adding 0.02 g of NiFe<sub>2</sub>O<sub>4</sub> NPs to a 25 ml conical flask containing 20 ml of Co(II) solution at room temperature. The initial Co(II) concentrations varied from 60 mg/l to 540 mg/l. The pH of the solution was adjusted to 2-10 using 0.1 mol/l HCl and/or 0.1 mol/l NaOH solutions. After adding NiFe<sub>2</sub>O<sub>4</sub> NPs, the flasks were transferred to a temperature controlled shaking water bath and shaken at 180 rpm for 24 hours. Then, the NiFe<sub>2</sub>O<sub>4</sub> NPs was separated using an external magnet and the concentration of the remaining Co(II) ions in the solution was determined through ICP-OES. The concentration of the remaining Co(II) ions in the adsorbent phase ( $q_e$ , mg/g) was calculated using equation (1):

$$q_e = \frac{(C_0 - C_e)V}{W} \quad (1)$$

where  $C_0$  and  $C_e$  (mg/l) are initial and equilibrium concentrations, respectively,  $V$  (l) is the volume of solution, and  $W$  (g) is the mass of the adsorbent.<sup>20</sup>

Finally, Co(II) ions removal efficiency was calculated using equation (2):

$$R (\%) = \frac{C_0 - C_e}{C_0} \times 100 \quad (2).$$

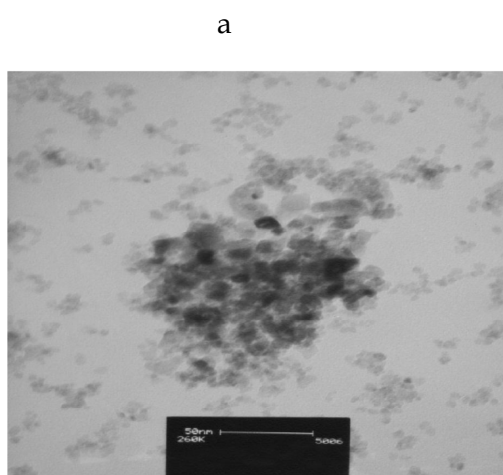
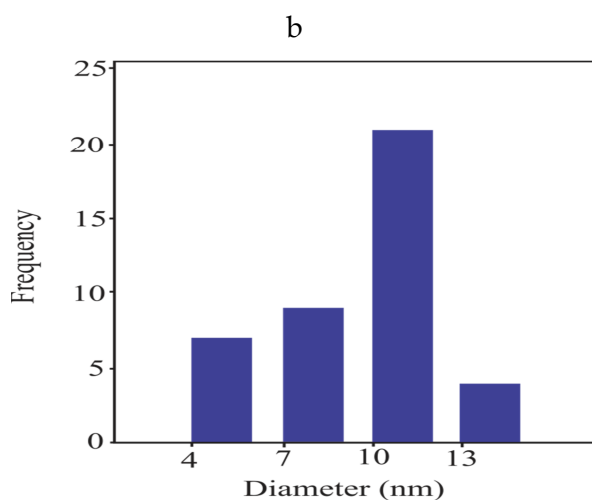


Figure 2. (a) Transmission electron micrograph and (b) calculated histogram of NiFe<sub>2</sub>O<sub>4</sub> nanoparticles



## Results and Discussion

### Characterization of NiFe<sub>2</sub>O<sub>4</sub>

The XRD pattern (Figure 1) shows that the peaks at the  $2\theta$  values of 30.1, 35.3, 43.0, 53.7, 56.5, and 62.4 can be assigned as (220), (311), (400), (422), (511), and (440) crystal planes of spinel NiFe<sub>2</sub>O<sub>4</sub>, respectively. The average crystallite size of the NiFe<sub>2</sub>O<sub>4</sub> NPs was estimated at 15 nm from the XRD data according to the Scherer equation. The TEM micrograph and calculated histogram of the NiFe<sub>2</sub>O<sub>4</sub>, as shown in figure 2, revealed that the diameter of the synthesized NiFe<sub>2</sub>O<sub>4</sub> NPs was around 12 nm.

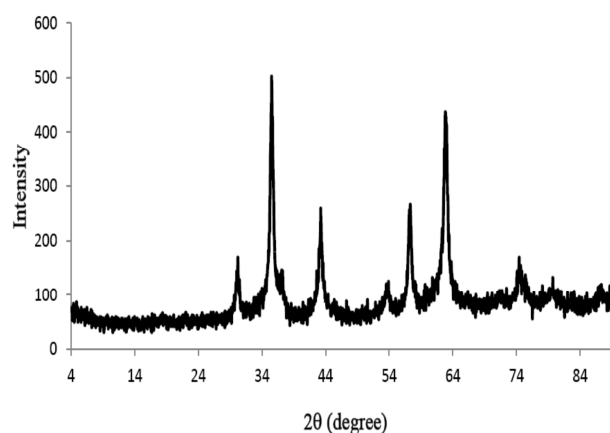


Figure 1. The X-ray diffraction pattern of NiFe<sub>2</sub>O<sub>4</sub> nanoparticles.

The particle size measured directly on the TEM micrograph is in accordance with that determined by the XRD results. Figure 3 shows a typical SEM-EDX elemental analysis of NiFe<sub>2</sub>O<sub>4</sub> NPs. The results demonstrate that only Ni, Fe, and O appear in NiFe<sub>2</sub>O<sub>4</sub> NPs samples. Moreover, the results have a good agreement with previous studies. Specific surface areas are commonly reported as Brunauer-Emmett-Teller (BET) surface areas obtained through applying the BET theory to nitrogen adsorption/desorption isotherms measured at 77 K. This is a standard procedure for the determination of the specific surface area of a sample. The specific surface area of the sample is determined by physical adsorption of a gas on the surface of the solid and by measuring the amount of adsorbed gas corresponding to a monomolecular layer on the surface. The data are treated according to the BET theory.<sup>21</sup> The results of the BET method showed that the average specific surface area of NiFe<sub>2</sub>O<sub>4</sub> NPs was 63.7 m<sup>2</sup>/g. It can be concluded from these values that the synthesized nanoparticles have relatively large specific surface areas and may be better for adsorption.

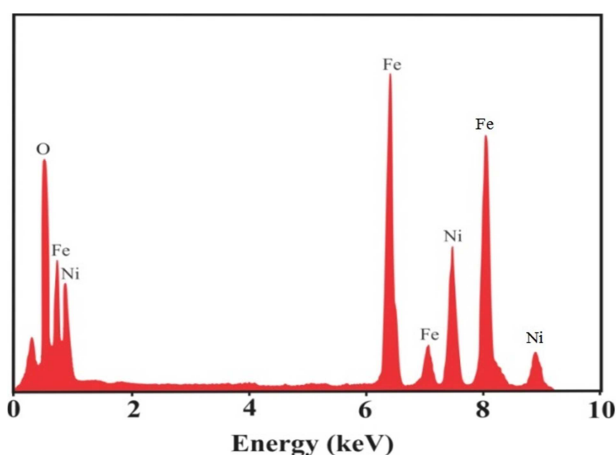


Figure 3. Scanning electron microscope energy dispersive X-ray spectrum of NiFe<sub>2</sub>O<sub>4</sub> nanoparticles

#### Effect of solution pH

The solution pH has an important impact on the active sites of adsorbent as well as the

metal speciation during the adsorption process. To evaluate the effect of pH on the adsorption percentage of the Co(II) ions, experiments were performed at initial concentration of 60 mg/l and pH range 2-10 (Figure 4b).

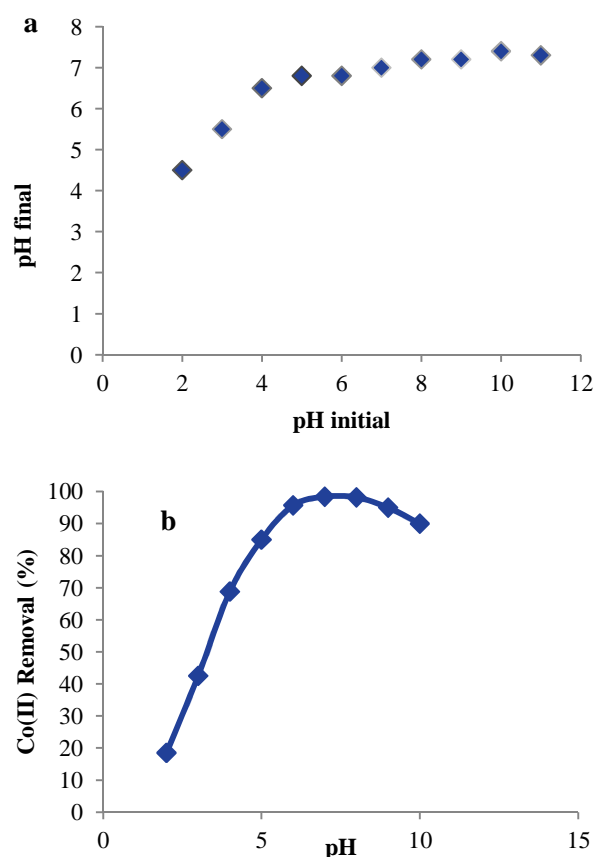


Figure 4. (a) The determination of the point of zero charge of the NiFe<sub>2</sub>O<sub>4</sub> nanoparticles (b) Effect of solution pH on the removal efficiency of Co(II) by NiFe<sub>2</sub>O<sub>4</sub> nanoparticles ( $C_0 = 60$  mg/l, contact time = 70 minutes, dose of adsorbent = 0.02 g, and temperature = 25 °C)

The Co(II) ions removal was found to increase significantly with increase in solution pH from pH of 2 to 7. The highest Co(II) ions removal (98.4%) was achieved at pH 7. This could be attributed to the surface properties of the adsorbent and ionization/dissociation of the adsorbate molecules. As observed in figure 4a, the  $pH_{pzc}$  for NiFe<sub>2</sub>O<sub>4</sub> NPs is 7.0. The concentration of H<sup>+</sup> ion increased gradually in

the system with the decrease of pH value and the NiFe<sub>2</sub>O<sub>4</sub> NPs surface became more positively charged because of the protonation of molecules on the NiFe<sub>2</sub>O<sub>4</sub> NPs surface. The increase in Co(II) ions removal with the increases in pH (> p*H*<sub>pzc</sub>) can be explained on the basis of a decrease in competition between protons and Co(II) cations for the same functional groups and by the decrease in positive surface charge, which results in a lower electrostatic repulsion between the surface of NiFe<sub>2</sub>O<sub>4</sub> NPs and Co(II) ions before adsorption.

Generally, various Co species in aqueous solution are present in the form of Co<sup>2+</sup>, Co(OH)<sup>+</sup>, Co(OH)<sub>2</sub>, and Co(OH)<sub>3</sub><sup>-</sup> at a function of pH values. At a pH of less than 9, the predominant cobalt species is Co<sup>2+</sup> and the removal of Co(II) is accomplished through the adsorption process. A similar phenomenon has also been shown in the adsorption of Co(II) ion from water by carboxylated sugarcane bagasse.<sup>1</sup>

#### Effect of adsorbent dose

Dose of adsorbent is an important parameter in the determination of adsorption capacity and adsorption efficiency. The effect of adsorbent amount on removal of Co(II) ions was investigated by adding various amounts of adsorbent in the range of 0.006-0.08 g and pH of 7 with initial metal concentration of 60 mg/l. The results are illustrated in figure 5. As can be seen, removal of Co(II) increases from 68% to 99.3% for 0.006-0.02 g. This could be attributed to the fact that by increasing the NiFe<sub>2</sub>O<sub>4</sub> NPs amount for the same concentration of Co(II) solution, the number of sites available for adsorption continue increasing. However, in the next stage, removal attained its maximum limit and further increase had no effect. Similar results were observed by Deravanesiyan et al. who investigated the effect of adsorbent dose on removal of Co(II) ions from aqueous solution by alumina nanoparticles immobilized zeolite and indicated that adsorption increases with increase in adsorbent dose.<sup>22</sup>

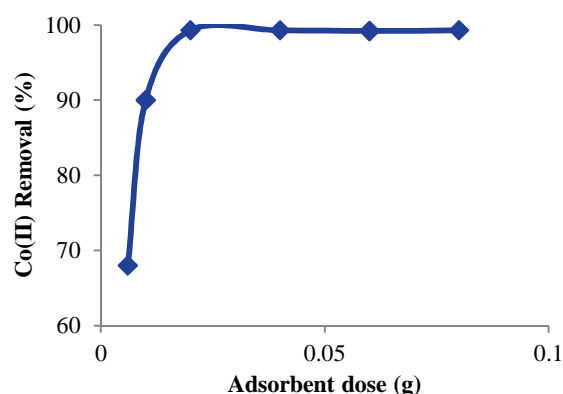


**Figure 5.** Effect of adsorbent dose on the removal efficiency of Co(II) by NiFe<sub>2</sub>O<sub>4</sub> nanoparticles (*C*<sub>0</sub> = 60 mg/l, solution pH = 7, contact time = 70 minutes, and temperature = 25 °C)

#### Effect of temperature

In order to study the effect of temperature, experiments were carried out at 25, 35, 45, and 55 °C and the results are presented in figure 6. The increase in the temperature of Co(II) solution from 25 to 55 °C resulted in a decrease in the adsorption efficiency of the NiFe<sub>2</sub>O<sub>4</sub> NPs. This indicates that the adsorption of Co(II) ions on NiFe<sub>2</sub>O<sub>4</sub> NPs is exothermic in nature. The decrease in adsorption with the increase in temperature may be attributed to the weakening of adsorptive forces between the active sites of the NiFe<sub>2</sub>O<sub>4</sub> NPs and Co(II) ions. Similar results have been found by Zandipak et al.<sup>19</sup>

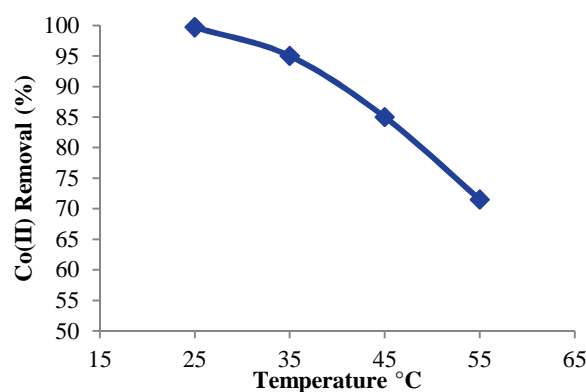


**Figure 6.** Effect of temperature on the removal efficiency of Co(II) by NiFe<sub>2</sub>O<sub>4</sub> nanoparticles (*C*<sub>0</sub> = 60 mg/l, solution pH = 7, dose of adsorbent = 0.02 g, contact time = 70 minutes, and temperature = 25 °C)



### Adsorption isotherms

Isotherms are the equilibrium relations between the adsorbate concentration in the solid phase and the liquid phase. The equilibrium isotherms for adsorption of Co(II) by NiFe<sub>2</sub>O<sub>4</sub> NPs were investigated with varying initial concentrations of Co(II) (from 60 to 540 mg/l) at 7.0 pH and 25 °C. The results indicate that adsorption is high at lower metal concentrations and decreases gradually with increase in metal concentration. In this study, the Langmuir [Equation (3)] and Freundlich [Equation (4)] isotherms were used to fit the adsorption data of Co(II) ions onto NiFe<sub>2</sub>O<sub>4</sub> NPs. The linear equations are as follows: <sup>23,24</sup>

$$\frac{C_e}{q_e} = \frac{C_e}{q_m} + \frac{1}{q_m b_1} \quad (3)$$

$$\ln q_e = \frac{1}{n} \ln C_e + \ln k_f \quad (4)$$

where  $C_e$  (mg/l) is the equilibrium concentration of Co(II) ions in solution,  $q_e$  (mg/g) is the equilibrium adsorption capacity of NiFe<sub>2</sub>O<sub>4</sub> NPs,  $q_m$  (mg/g) is the maximum adsorption capacity of NiFe<sub>2</sub>O<sub>4</sub> NPs for monolayer coverage,  $b$  (l/mg) is a constant related to the adsorption free energy,  $K_f$  (mg<sup>1/(1/n)</sup>l<sup>1/n</sup>/g) is a constant related to adsorption capacity, and  $n$  is an empirical parameter related to adsorption. The parameters of the isotherm equations for Co(II) ions on the NiFe<sub>2</sub>O<sub>4</sub> NPs are presented in table 1. As seen in table 1, the R<sup>2</sup> values obtained from the Langmuir model are much closer to one than those from the Freundlich model, suggesting that the Langmuir model is better than the other isotherms (Figure 7). Thus, the adsorption can be described by the Langmuir isotherm and the Co(II) ions adsorption occurs

on a homogeneous surface through monolayer adsorption without interaction between the adsorbed ions. Through the comparison of  $q_{max}$  values of Co(II) adsorption capacity of other adsorbents to NiFe<sub>2</sub>O<sub>4</sub> NPs (Table 2), it is evident that NiFe<sub>2</sub>O<sub>4</sub> NPs presented the highest adsorption capacity of the reported adsorbents.

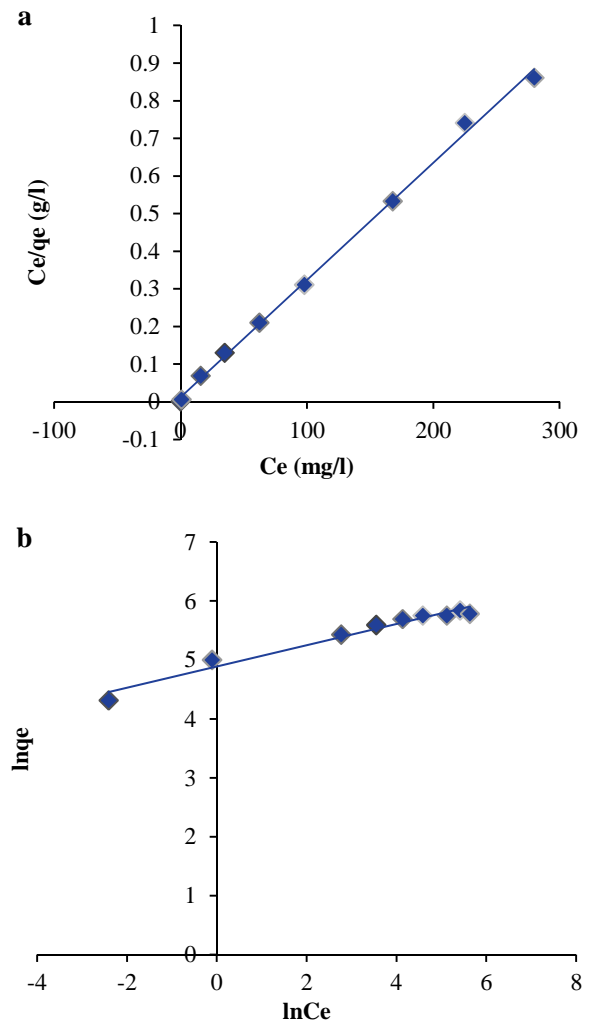


Figure 7. (a) Langmuir and (b) Freundlich isotherms for Co(II) ions adsorption onto NiFe<sub>2</sub>O<sub>4</sub> nanoparticles

Table 1. Isotherm parameters of adsorption of Co(II) ions onto NiFe<sub>2</sub>O<sub>4</sub> nanoparticles at 25 °C

Langmuir			Freundlich		
b (l mg <sup>-1</sup> )	q <sub>m</sub> (mg g <sup>-1</sup> )	R <sup>2</sup>	K <sub>f</sub> (mg <sup>1-(1/n)</sup> l <sup>1/n</sup> g <sup>-1</sup> )	n	R <sup>2</sup>
0.265	322.5	0.997	132.55	5.54	0.967

q<sub>m</sub>: Maximum adsorption capacity; R<sup>2</sup>: Pearson correlation coefficient; K<sub>f</sub>: Freundlich constant related to adsorption capacity; n: Empirical parameter related to adsorption

**Table 2. Comparison of maximum adsorption capacity (q<sub>m</sub>) of different adsorbents for Co(II)**

Adsorbent	Maximum adsorption capacity (mg/g)	Reference
Amination graphene oxide	116.30	2
Alumina nanoparticles immobilized zeolite	5.05	22
Nano-magnesso ferrite	62.68	5
Chrysanthemum indicum	14.84	25
Granular activated carbon	1.19	26
Chelating resin	71.29	6
NiFe <sub>2</sub> O <sub>4</sub> nanoparticles	322.50	This work

### Adsorption kinetics

The adsorption of Co(II) ions by NiFe<sub>2</sub>O<sub>4</sub> NPs as a function of time at three different initial Co(II) concentrations (60, 80, and 120 mg/l) is displayed in figure 8. As can be observed, the adsorption efficiency of Co(II) ions increased with increasing contact time, and finally, reached equilibrium after approximately 70 minutes. A rapid adsorption was observed within 50 minutes which showed the availability of a large number of vacant sites. Subsequently, the diminishing availability of the remaining active sites and the decrease in the driving force led to the slowing of the adsorptive process.

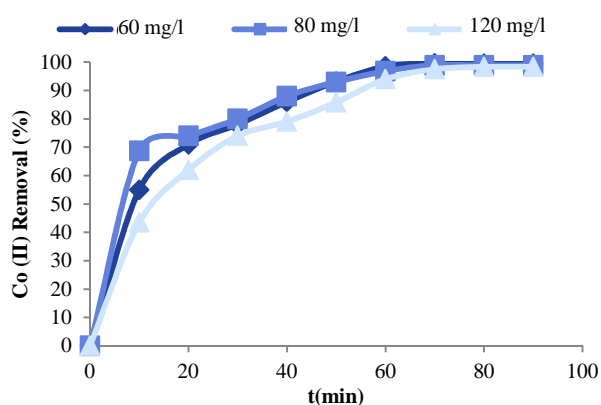


**Figure 8. Effect of contact time on the removal efficiency of Co(II) by NiFe<sub>2</sub>O<sub>4</sub> nanoparticles (C<sub>0</sub> = 60, 80 and 120 mg/l, solution pH = 7, dose of adsorbent = 0.02 g, and temperature = 25 °C)**

To evaluate the kinetics of the adsorption process, the experimental data were compared to those predicted by two kinetic models, the pseudo-first order and pseudo-second order.

The pseudo-first order and pseudo-second order kinetic models can, respectively, be expressed by equation (5) and (6):<sup>27</sup>

$$\ln(q_e - q_t) = \ln(q_e) - \frac{k_1 t}{2.303} \quad (5)$$

$$\frac{t}{q_t} = \frac{1}{k_2 q_e^2} + \frac{t}{q_e} \quad (6)$$

where  $q_e$  and  $q_t$  are the amount of Co(II) ions adsorbed (mg/g) at equilibrium and time  $t$  (minute),  $k_1$  is the rate constant of pseudo-first order (minute<sup>-1</sup>),  $k_2$  is the rate constant of pseudo-second order (g/mg/minute) for adsorption. The pseudo-first order and pseudo-second order kinetics plots are presented in figure 9. The kinetic constants and correlation coefficients of these two models are calculated and given in table 3. The results show that the correlation coefficients ( $R^2$ ) (0.998, 0.998, and 0.997) for the pseudo-second order models are higher than the pseudo-first order models (0.923, 0.851, and 0.838). This indicates that the adsorption of Co(II) ions on NiFe<sub>2</sub>O<sub>4</sub> NPs follows a pseudo-second order kinetic model. The results indicate that chemical adsorption might be the rate-limiting step.

### Conclusion

In this work, NiFe<sub>2</sub>O<sub>4</sub> NPs were successfully synthesized and used as a novel adsorbent for the rapid individual adsorption of Co(II) ions. The size of the nanostructures, according to TEM, was around 12 nm. The NiFe<sub>2</sub>O<sub>4</sub> NPs can be easily separated from the aqueous solution by the external magnetic field before and after the adsorption process. The results indicate

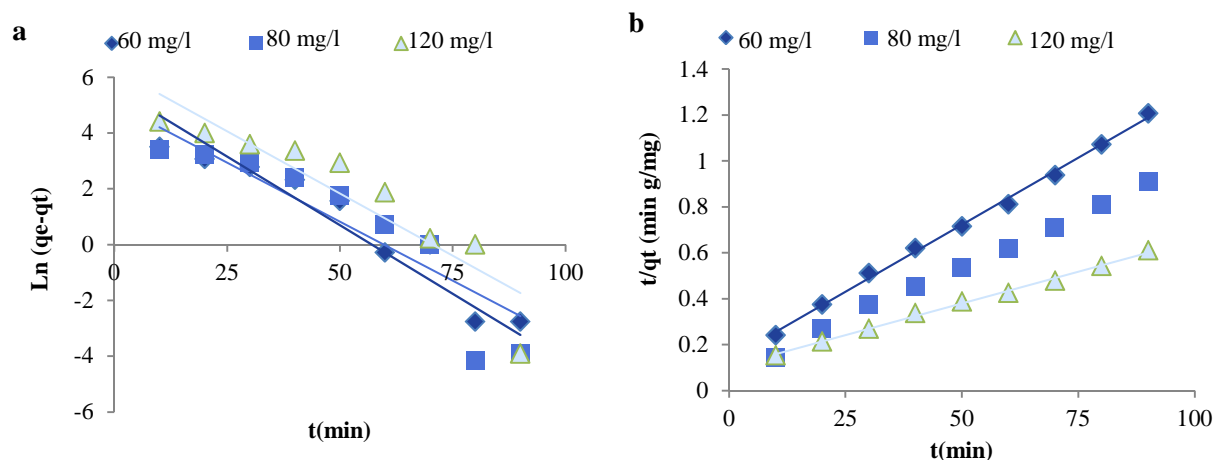


Figure 9. (a) Pseudo-first order and (b) pseudo-second order kinetics plots of Co(II) ions adsorption onto NiFe<sub>2</sub>O<sub>4</sub> nanoparticles

Table 3. Pseudo-first order and pseudo-second order kinetic model parameters for the adsorption of Co(II) ions onto NiFe<sub>2</sub>O<sub>4</sub> nanoparticles at 25 °C

C <sub>0</sub> (mg/l)	Pseudo-first order kinetic model				Pseudo-second order kinetic model		
	q <sub>e</sub> exp (mg/g)	q <sub>e1</sub> (mg/g)	k <sub>1</sub> (minute <sup>-1</sup> )	R <sup>2</sup>	q <sub>e2</sub> (mg/g)	k <sub>2</sub> (g/mg/minute)	R <sup>2</sup>
60	56.0	21.40	0.09	0.923	54.21	0.020	0.998
80	73.4	67.25	0.08	0.851	72.95	0.010	0.998
120	107.8	84.65	0.03	0.838	105.7	0.005	0.997

q<sub>e</sub>: Amount of Co(II) ions adsorbed at equilibrium; k<sub>1</sub>: Rate constant of pseudo-first order; R<sup>2</sup>: Pearson correlation coefficient; k<sub>2</sub>: Rate constant of pseudo-second order for adsorption

that the adsorption was dependent on the pH of solution and temperature. The adsorption kinetics and adsorption isotherms showed that the adsorption kinetic could be modeled by the pseudo-second order rate equation, and the isotherm equilibrium data were well fitted with the Langmuir model. The adsorption capacity of Co(II) onto NiFe<sub>2</sub>O<sub>4</sub> NPs was determined as 322.5 mg/g. Thus, NiFe<sub>2</sub>O<sub>4</sub> NPs can potentially be used to treat Co(II)-contaminated wastewater.

### Conflict of Interests

Authors have no conflict of interests.

### Acknowledgements

The authors are very grateful to the Young Researchers and Elite Club, Hamedan Branch, Islamic Azad University for providing us with facilities to conduct and complete this study.

### References

1. Carmo Ramos S, Pedrosa Xavier A, Teodoro F, Cota Elias M, Jorge Goncalves F, Frederic Gil L, et al. Modeling mono- and multi-component adsorption of cobalt(II), copper(II), and nickel(II) metal ions from aqueous solution onto a new carboxylated sugarcane bagasse. Part I: Batch adsorption study. *Industrial Crops and Products* 2015; 74: 357-71.
2. Fang F, Kong L, Huang J, Wu S, Zhang K, Wang X, et al. Removal of cobalt ions from aqueous solution by an amination graphene oxide nanocomposite. *J Hazard Mater* 2014; 270: 1-10.
3. Nazari AM, Cox PW, Waters KE. Biosorption of copper, nickel and cobalt ions from dilute solutions using BSA-coated air bubbles. *Journal of Water Process Engineering* 2014; 3: 10-7.
4. Negm NA, El Sheikh R, El-Faragy AF, Hefni Hassan H, Bekhit M. Treatment of industrial wastewater containing copper and cobalt ions using modified chitosan. *Journal of Industrial and Engineering Chemistry* 2015; 21: 526-34.
5. Srivastava V, Sharma YC, Sillanpaa M. Application of nano-magnesso ferrite (n-MgFe<sub>2</sub>O<sub>4</sub>) for the removal of Co<sup>2+</sup> ions from synthetic wastewater: Kinetic, equilibrium and thermodynamic studies.



- Applied Surface science 2015; 338: 42-54.
- Ceglowski M, Schroeder G. Preparation of porous resin with Schiff base chelating groups for removal of heavy metal ions from aqueous solutions. *Chemical Engineering Journal* 2015; 263: 402-11.
  - Zhu J, Baig SA, Sheng T, Lou Z, Wang Z, Xu X. Fe<sub>3</sub>O<sub>4</sub> and MnO<sub>2</sub> assembled on honeycomb briquette cinders (HBC) for arsenic removal from aqueous solutions. *J Hazard Mater* 2015; 286: 220-8.
  - Jian M, Liu B, Zhang G, Liu R, Zhang X. Adsorptive removal of arsenic from aqueous solution by zeolitic imidazolate framework-8 (ZIF-8) nanoparticles. *Colloids and Surfaces A: Physicochem Eng Aspects* 2015; 465: 67-76.
  - Arshadi M, Faraji AR, Amiri MJ. Modification of aluminum silicate nanoparticles by melamine-based dendrimer l-cysteine methyl esters for adsorptive characteristic of Hg(II) ions from the synthetic and Persian Gulf water. *Chemical Engineering Journal* 2015; 266: 345-55.
  - Sobhanardakani S, Zandipak R, Sahraei R. Removal of Janus Green dye from aqueous solutions using oxidized multi-walled carbon nanotubes. *Toxicol Environ Chem* 2013; 95(6): 909-18.
  - Ahmad MA, Alrozi R. Removal of malachite green dye from aqueous solution using rambutan peel-based activated carbon: Equilibrium, kinetic and thermodynamic studies. *Chemical Engineering Journal* 2011; 171(2): 510-6.
  - Ghaedi M, Mosallanejad N. Study of competitive adsorption of malachite green and sunset yellow dyes on cadmium hydroxide nanowires loaded on activated carbon. *Journal of Industrial and Engineering Chemistry* 2014; 20(3): 1085-96.
  - Sun Q, Hu X, Zheng S, Sun Z, Liu S, Li H. Influence of calcination temperature on the structural, adsorption and photocatalytic properties of TiO<sub>2</sub> nanoparticles supported on natural zeolite. *Powder Technology* 2015; 274: 88-97.
  - Wan Ngah WS, Teong LC, Hanafiah MA. Adsorption of dyes and heavy metal ions by chitosan composites: A review. *Carbohydrate Polymers* 2011; 83(4): 1446-56.
  - Yu L, Luo YM. The adsorption mechanism of anionic and cationic dyes by Jerusalem artichoke stalk-based mesoporous activated carbon. *Journal of Environmental Chemical Engineering* 2014; 2(1): 220-9.
  - Teymourian H, Salimi A, Khezrian S. Fe<sub>3</sub>O<sub>4</sub> magnetic nanoparticles/reduced graphene oxide nanosheets as a novel electrochemical and bioelectrochemical sensing platform. *Biosensors and Bioelectronics* 2013; 49: 1-8.
  - Khosravi I, Eftekhari M. Characterization and evaluation catalytic efficiency of NiFe<sub>2</sub>O<sub>4</sub> nano spinel in removal of reactive dye from aqueous solution. *Powder Technology* 2013; 250: 147-53.
  - Patil JY, Nadargi DY, Gurav JL, Mulla IS, Suryavanshi SS. Synthesis of glycine combusted NiFe<sub>2</sub>O<sub>4</sub> spinel ferrite: A highly versatile gas sensor. *Materials Letters* 2014; 124: 144-7.
  - Zandipak R, Sobhanardakani S. Synthesis of NiFe<sub>2</sub>O<sub>4</sub> nanoparticles for removal of anionic dyes from aqueous solution. *Desalination and Water Treatment* 2016; 57: 24-11348.
  - Wang XS, Zhu L, Lu HJ. Surface chemical properties and adsorption of Cu (II) on nanoscale magnetite in aqueous solutions. *Desalination* 2011; 276(1-3): 154-60.
  - Brunauer S, Emmett PH, Teller E. Adsorption of Gases in Multimolecular Layers. *J Am Chem Soc* 1938; 60(2): 309-19.
  - Deravanesian M, Beheshti M, Malekpour A. Alumina nanoparticles immobilization onto the NaX zeolite and the removal of Cr (III) and Co (II) ions from aqueous solutions. *Journal of Industrial and Engineering Chemistry* 2015; 21: 580-6.
  - Langmuir L. The adsorption of gases on plane surfaces of glass, mica and platinum. *J Am Chem Soc* 1918; 40(9): 1361-403.
  - Freundlich H, Heller W. The Adsorption of cis- and trans-Azobenzene. *J Am Chem Soc* 1939; 61(8): 2228-30.
  - Vilvanathan S, Shanthakumar S. Biosorption of Co(II) ions from aqueous solution using *Chrysanthemum indicum*: Kinetics, equilibrium and thermodynamics. *Process Safety and Environmental Protection* 2015; 96: 98-110.
  - Sulaymon AH, Abid BA, Al-Najar JA. Removal of lead copper chromium and cobalt ions onto granular activated carbon in batch and fixed-bed adsorbers. *Chemical Engineering Journal* 2009; 155(3): 647-53.
  - Azizian S. Kinetic models of sorption: a theoretical analysis. *J Colloid Interface Sci* 2004; 276(1): 47-52.